Asynchronous Performance Analysis of a Single-Phase Capacitor-Start, Capacitor-Run Permanent Magnet Motor

Mircea Popescu, *Senior Member, IEEE*, T. J. E. Miller, *Fellow, IEEE*, Malcolm McGilp, Giovanni Strappazzon, Nicolla Trivillin, and Roberto Santarossa

***Abstract*—This paper presents a detailed analysis of the asynchronous torque components (average cage, magnet braking torque and pulsating) for a single-phase capacitor-start, capacitor-run permanent magnet motor. The computed envelope of pulsating torque superimposed over the average electromagnetic torque leads to an accurate prediction of starting torque. The developed approach is realized by means of a combination of symmetrical components and *d-q* axes theory and it can be extended for any m-phase AC motor – induction, synchronous reluctance or synchronous permanent magnet. The resultant average electromagnetic torque is determined by superimposing the asynchronous torques and magnet braking torque effects.**

***Index Terms*—AC motors, capacitor motors, permanent magnet motors, starting, torque simulation.**

NOMENCLATURE

$\underline{V}_{\rm m}$, $\underline{V}_{\rm a}$	Complex voltage across main and auxiliary windings.
$\underline{V}_{+,-}$ $\underline{Z}_{+,-}$	Complex positive/negative sequence voltage and impedance.
$\underline{V}_{\rm d,q}$, $\underline{I}_{\rm d,q}$	Complex d-q axis voltage/current components in rotor reference frame.
$R_{\rm s}$, $R_{\rm a}$, $R_{\rm m}$	Stator winding resistance: equivalent/auxiliary/main.
$X_{\rm ls}X_{\rm la}$, $X_{\rm lm}$	Stator leakage reactance: equivalent/auxiliary/main.
β	Effective turns ratio (main/aux).
$R_{\rm rd}$, $R_{\rm rq}$	Rotor resistance for d-q axis.
$X_{\rm lrd}$, $X_{\rm lrq}$	Rotor leakage reactance for d-q axis.
$X_{\rm md}$, $X_{\rm mq}$	Magnetization reactance for d-q axis.
$\underline{X}_{\rm d\pm}$, $\underline{X}_{\rm q\pm}$	Complex positive/negative asynchronous reactance for *d-q* axis.
$X_{\rm d}$, $X_{\rm q}$	Synchronous reactance for d-q axis.
$\underline{Z}_{\rm C}$	Capacitive impedance connected in series with auxiliary winding.
m, P	Phases and poles number.
ω, s	Synchronous speed [rad/sec] and slip.

Manuscript received August 21, 2002; revised September 30, 2003. This work was supported by companies associated with *SPEED Consortium*.

M. Popescu, T. J. E. Miller, and M. I. McGilp are with SPEED Laboratory, Glasgow University, Glasgow G12 8LT, U.K. (e-mail: mircea@elec.gla.ac.uk; t.miller@elec.gla.ac.uk; mal@elec.gla.ac.uk).

G. Strappazzon, N. Trivillin, and R. Santarossa are with the Zanussi Elettromeccanica, Comina 33170, Italy (e-mail: giovanni.strappazzon@electrolux.it; nicola.trivillin@electrolux.it; roberto.santarossa@electrolux.it).

Digital Object Identifier 10.1109/TEC.2004.837307

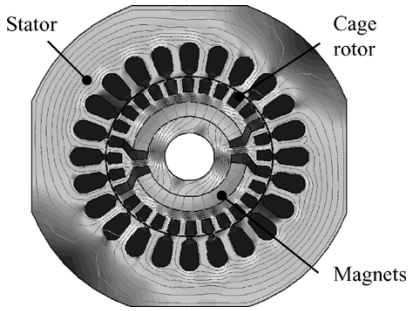

Fig. 1. Cross-section of analyzed motor with load operation flux-lines.

E_0	No-load induced voltage.
$N_{\rm m}$	Number of turns on main stator winding.
$\rm d_{m,a}$	Wire diameter of the main/auxiliary winding.

I. INTRODUCTION

THIS WORK aims to extend the existing analysis made at asynchronous operation for a single-phase unsymmetrical [1], [2] and for a three-phase symmetrical line-start permanent magnet motor (LSPMM) [4]. In addition to [1], [2] this paper presents a detailed theoretical approach on how the asynchronous (cage and magnet braking) torques are to be computed, emphasising the advantages and limitations of the proposed analytical method. The analysis focuses on a single-phase capacitor-start, capacitor-run, 50 Hz two-pole motor with sine-distributed concentric windings. The rotor consists of an aluminum rotor cage, with arc-shaped interior ferrite magnets, Fig. 1.

LSPMMs start asynchronously like induction motor and run synchronously as any other synchronous motor type. The capacitor-start, capacitor-run permanent magnet motor is the single-phase version of the LSPM motor. This special electric motor is suited for application in home appliances, such as refrigerator compressors [1], [2].

The induced currents in the rotor bars during the asynchronous operation will interact with the stator flux-linkages and a *cage torque* will be produced. This torque ensures the starting capabilities of LSPMM.

However, the permanent magnetization of the rotor makes starting more difficult. Current generated by the rotating magnets causes a Joule loss in the stator circuit resistance, which results in a drag torque or *magnet braking torque*, [1], [2], [4], [6], [16]. Torque oscillations during starting are not only higher, but also persist longer than those in the induction motor. The DC

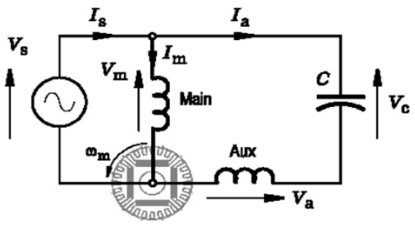

Fig. 2. Circuit for analysis of LSPM motor with capacitor connection.

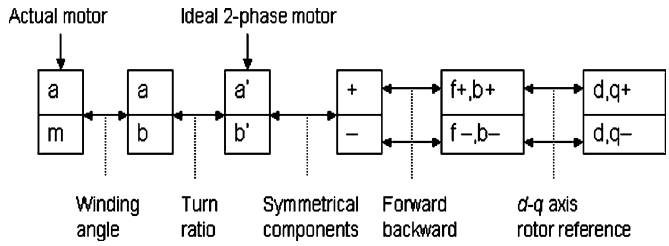

Fig. 3. Transformation from actual voltages and currents to d-q axis quantities for LSPM motor.

offset responsible for transient oscillatory torque in the induction motor decays according to the rotor time-constant, but the permanent magnet sustains a nondecaying offset flux that causes oscillatory torques that persist until the motor has synchronized. In single-phase motors, where the auxiliary winding is supplied through a capacitor, the operation is further complicated by the imbalance between the main and auxiliary winding voltages and that the cage rotor losses are expected to be minimized at nominal load.

For steady-state (synchronous) operation of such motors permanent magnets provide an increased electromagnetic torque. A detailed approach to different torque components (average and pulsating) for a single-phase capacitor-start, capacitor-run permanent magnet motor permits a correct estimation of motor performance.

The traditional way to study the asynchronous starting process of a LSPMM is to divide it into two different regions [4]–[10], [31]: a) the run-up response up to the "rated induction motor operation point", where the accelerating torque is given by the cage torque minus the magnet braking torque and load torque; b) the transition zone from that point to synchronism.

This paper analyzes the motor operation in the first region.

II. The Asynchronous Cage Torques

The unbalanced stator voltage for the case of capacitor- start and/or -run motors affects both the starting and synchronous operation. For a detailed analysis of the torque behavior, a suitable combination of the symmetrical components and d-q axis theory [1]–[3], [30] will give accurate results. The variables are expressed as space vectors using complex numbers. Fig. 2 shows the circuit for analysis of the LSPMM when a capacitive impedance is series connected with the auxiliary winding. Fig. 3 illustrates the necessary transformations from the actual variables to the proposed model variables.

The stator windings are assumed to have the same copper weight and distribution, i.e., $R_s = R_m = \beta^2 R_a$, $X_{ls} = X_{lm} = \beta^2 X_{la}$, $d_a = \beta^{1/2} d_m$. Considering the stator windings are magnetically orthogonal we can write the transformation between the actual motor parameters and ideal 2-phase motor as

$$\begin{bmatrix} \underline{V}'_a \\ \underline{V}'_b \end{bmatrix} = \begin{bmatrix} 1 & 0 \\ 0 & \frac{1}{\beta} \end{bmatrix} \cdot \begin{bmatrix} \underline{V}_a \\ \underline{V}_m \end{bmatrix} \tag{1}$$

$$\begin{bmatrix} \underline{I}'_a \\ \underline{I}'_b \end{bmatrix} = \begin{bmatrix} 1 & 0 \\ 0 & \beta \end{bmatrix} \cdot \begin{bmatrix} \underline{I}_a \\ \underline{I}_m \end{bmatrix}. \tag{2}$$

The circuit in Fig. 2 is constrained by the equation

$$\underline{V}_s = \underline{V}_m = \underline{V}_a + \underline{Z}_C \cdot \underline{I}_a. \tag{3}$$

The symmetrical components $\underline{V}_+, \underline{V}_-, \underline{I}_+, \underline{I}_-$ are introduced by the following transformation matrix equation from the balanced machine $[a', b']$ machine considering an invariant magnitude:

$$\begin{bmatrix} \underline{V}_+ \\ \underline{V}_- \end{bmatrix} = \frac{1}{2} \begin{bmatrix} 1 & j \\ 1 & -j \end{bmatrix} \cdot \begin{bmatrix} \underline{V}'_a \\ \underline{V}'_b \end{bmatrix} \tag{4}$$

with inverse

$$\begin{bmatrix} \underline{V}'_a \\ \underline{V}'_b \end{bmatrix} = \begin{bmatrix} 1 & 1 \\ -j & j \end{bmatrix} \cdot \begin{bmatrix} \underline{V}_+ \\ \underline{V}_- \end{bmatrix}. \tag{5}$$

The same transformation may be applied to the currents. Substituting from (1), (2), (4) in (3) we get

$$\underline{V}_+ = \underline{V}_m \cdot \frac{1}{\beta} \cdot \frac{\beta + j\underline{a}_2}{\underline{a}_1 + \underline{a}_2} \tag{6}$$

$$\underline{V}_- = \underline{V}_m \cdot \frac{1}{\beta} \cdot \frac{\beta - j\underline{a}_1}{\underline{a}_1 + \underline{a}_2} \tag{7}$$

and

$$\underline{V}_+ = \underline{Z}_+ \cdot \underline{I}_+ \tag{8}$$

$$\underline{V}_- = \underline{Z}_- \cdot \underline{I}_- \tag{9}$$

where underscores stand for complex variables and

$$\underline{a}_1 = 1 + \frac{\underline{Z}_C}{\underline{Z}_+} \tag{10}$$

$$\underline{a}_2 = 1 + \frac{\underline{Z}_C}{\underline{Z}_-}. \tag{11}$$

The presence of the capacitive impedance connected in series with the auxiliary winding requires a special usage of the symmetrical components. A suitable option is to include the capacitor voltage in the positive and negative sequence voltages. The positive and negative sequence impedances are approximated using the average of the d and q-axis impedances

$$\underline{Z}_+ = R_s + jX_{ls} + \frac{1}{2} \cdot \left[\begin{array}{l} \frac{jX_{md} \cdot \left(\frac{R_{rd}}{s} + jX_{lrd}\right)}{\frac{R_{rd}}{s} + j \cdot (X_{md} + X_{lrd})} + \\ \frac{jX_{mq} \cdot \left(\frac{R_{rq}}{s} + jX_{lrq}\right)}{\frac{R_{rq}}{s} + j \cdot (X_{mq} + X_{lrq})} \end{array} \right] \tag{12}$$

$$\underline{Z}_- = R_s + jX_{ls} + \frac{1}{2} \cdot \left[\begin{array}{l} \frac{jX_{md} \cdot \left(\frac{R_{rd}}{2-s} + jX_{lrd}\right)}{\frac{R_{rd}}{2-s} + j \cdot (X_{md} + X_{lrd})} + \\ \frac{jX_{mq} \cdot \left(\frac{R_{rq}}{2-s} + jX_{lrq}\right)}{\frac{R_{rq}}{2-s} + j \cdot (X_{mq} + X_{lrq})} \end{array} \right]. \tag{13}$$

The unbalanced supply voltage system can be further decomposed into an orthogonal system (d-q) using symmetrical components as [3]

$$\underline{V}_{\mathrm{d}} = \left(\underline{V}_{+} + \underline{V}_{-}\right) = \left(\underline{V}_{\mathrm{d}+} + \underline{V}_{\mathrm{d}-}\right) \tag{14}$$

$$\underline{V}_{\mathrm{q}} = \left(-j\underline{V}_{+} + j\underline{V}_{-}\right) = \left(\underline{V}_{\mathrm{q}+} + \underline{V}_{\mathrm{q}-}\right). \tag{15}$$

The positive sequence $\underline{V}_{+}$ will induce currents in the cage rotor of the LSPM motor. If f is the fundamental supply frequency, the frequency of the rotor currents will be sf. In a similar way, the negative sequence $\underline{V}_{-}$ will induce currents in the cage rotor, with frequency $(2-s)f$. In double revolving field theory, currents with frequency sf determine the forward field, and the currents of frequency $(2-s)f$ determine the backward field. Thus, the initial unbalanced LSPM motor is equivalent to two stator-balanced motors. Each of these fictitious motors is characterized by an asymmetrical rotor configuration, due to the cage and the permanent magnets.

Using the d-q axis fixed on the rotor frame, we can write the following linear differential stator voltage equations for the positive sequence motor [3]:

$$\underline{V}_{\mathrm{d}+} = \underline{V}_{+} = R_{\mathrm{s}}\underline{I}_{\mathrm{d}+} + js\omega\underline{\psi}_{\mathrm{d}+} - (1-s)\omega\underline{\psi}_{\mathrm{q}+} \tag{16}$$

$$\underline{V}_{\mathrm{q}+} = -j\underline{V}_{+} = R_{\mathrm{s}}\underline{I}_{\mathrm{q}+} + js\omega\underline{\psi}_{\mathrm{q}+} + (1-s)\omega\underline{\psi}_{\mathrm{d}+} \tag{17}$$

and for the negative sequence motor

$$\underline{V}_{\mathrm{d}-} = \underline{V}_{-} = R_{\mathrm{s}}\underline{I}_{\mathrm{d}-} + j(2-s)\omega\underline{\psi}_{\mathrm{d}-} - (1-s)\omega\underline{\psi}_{\mathrm{q}-} \tag{18}$$

$$\underline{V}_{\mathrm{q}-} = j\underline{V}_{-} = R_{\mathrm{s}}\underline{I}_{\mathrm{q}-} + j(2-s)\omega\underline{\psi}_{\mathrm{q}-} + (1-s)\omega\underline{\psi}_{\mathrm{d}-}. \tag{19}$$

For the flux linkage components we will use the notations [3]

$$\omega\underline{\psi}_{\mathrm{d}\pm} = \underline{X}_{\mathrm{d}\pm}(js)\underline{I}_{\mathrm{d}\pm} = -j\underline{Z}_{\mathrm{d}\pm}\underline{I}_{\mathrm{d}\pm} \tag{20}$$

$$\omega\underline{\psi}_{\mathrm{q}\pm} = \underline{X}_{\mathrm{q}\pm}(js)\underline{I}_{\mathrm{q}\pm} = -j\underline{Z}_{\mathrm{q}\pm}\underline{I}_{\mathrm{q}\pm}. \tag{21}$$

Introducing (20) and (21) in (14), (15) and respectively in (16), (17) and solving the equation systems, we may obtain the equivalent relations for d-q axis currents.

Positive sequence

$$\underline{I}_{\mathrm{d}+} = \frac{j\underline{V}_{+}}{D_{+}} \cdot \left[-R_{\mathrm{s}} + j(2s-1)\underline{X}_{\mathrm{q}+}\right] \tag{22}$$

$$\underline{I}_{\mathrm{q}+} = -\frac{\underline{V}_{+}}{D_{+}} \cdot \left[-R_{\mathrm{s}} + j(2s-1)\underline{X}_{\mathrm{d}+}\right]. \tag{23}$$

Negative sequence

$$\underline{I}_{\mathrm{d}-} = \frac{\underline{V}_{-}}{D_{-}} \cdot \left[R_{\mathrm{s}} + j(3-2s)\underline{X}_{\mathrm{q}-}\right] \tag{24}$$

$$\underline{I}_{\mathrm{q}-} = \frac{j\underline{V}_{-}}{D_{-}} \cdot \left[R_{\mathrm{s}} + j(3-2s)\underline{X}_{\mathrm{d}-}\right] \tag{25}$$

where

$$D_{+} = R_{\mathrm{s}}^2 + (1-2s)\underline{X}_{\mathrm{d}+}\underline{X}_{\mathrm{q}+} + jsR_{\mathrm{s}}\left(\underline{X}_{\mathrm{d}+} + \underline{X}_{\mathrm{q}+}\right) \tag{26}$$

$$D_{-} = R_{\mathrm{s}}^2 + (2s-3)\underline{X}_{\mathrm{d}-}\underline{X}_{\mathrm{q}-} + j(2-s)R_{\mathrm{s}}\left(\underline{X}_{\mathrm{d}-} + \underline{X}_{\mathrm{q}-}\right) \tag{27}$$

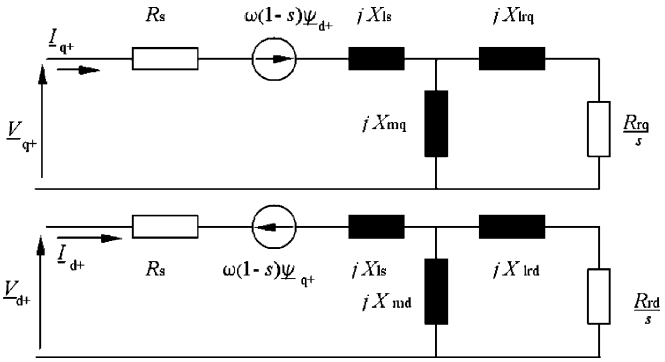

Fig. 4. LSPM motor positive sequence equivalent circuit for cage torque computation – fundamental mmf.

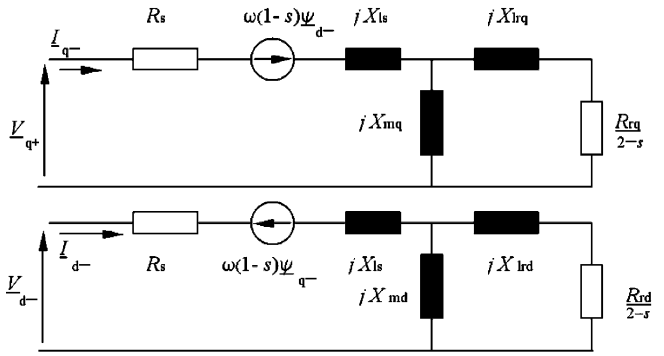

Fig. 5. LSPM motor negative sequence equivalent circuit for cage torque computation – fundamental mmf.

and

$$\underline{Z}_{\mathrm{d}\pm} = j\underline{X}_{\mathrm{d}\pm} = \underline{Z}_{\mathrm{md}\pm} + jX_{\mathrm{ls}} \tag{28}$$

$$\underline{Z}_{\mathrm{q}\pm} = j\underline{X}_{\mathrm{q}\pm} = \underline{Z}_{\mathrm{mq}\pm} + jX_{\mathrm{ls}} \tag{29}$$

while the equivalent d, q-axis magnetization impedances are

$$\underline{Z}_{\mathrm{md}+} = \frac{1}{\frac{1}{jX_{\mathrm{md}}} + \frac{s}{R_{\mathrm{rd}} + j\cdot sX_{\mathrm{lrd}}}} \tag{30}$$

$$\underline{Z}_{\mathrm{mq}+} = \frac{1}{\frac{1}{jX_{\mathrm{mq}}} + \frac{s}{R_{\mathrm{rq}} + j\cdot sX_{\mathrm{lrq}}}} \tag{31}$$

$$\underline{Z}_{\mathrm{md}-} = \frac{1}{\frac{1}{jX_{\mathrm{md}}} + \frac{(2-s)}{R_{\mathrm{rd}} + j\cdot(2-s)X_{\mathrm{lrd}}}} \tag{32}$$

$$\underline{Z}_{\mathrm{mq}-} = \frac{1}{\frac{1}{jX_{\mathrm{mq}}} + \frac{(2-s)}{R_{\mathrm{rq}} + j\cdot(2-s)X_{\mathrm{lrq}}}}. \tag{33}$$

A. Asynchronous Cage Torques

The following relations compute the air-gap average asynchronous cage torque components (positive and negative sequence) valid for a 1-phase AC motor with unbalanced stator voltage

$$T_{(\mathrm{cage})+} = \frac{P}{2} \cdot \mathrm{Re}\left\{\left(\underline{\psi}_{\mathrm{q}+}\right)^{*}\underline{I}_{\mathrm{d}+} - \left(\underline{\psi}_{\mathrm{d}+}\right)^{*}\underline{I}_{\mathrm{q}+}\right\} \tag{34}$$

$$T_{(\mathrm{cage})-} = \frac{P}{2} \cdot \mathrm{Re}\left\{\left(\underline{\psi}_{\mathrm{q}-}\right)^{*}\underline{I}_{\mathrm{d}-} - \left(\underline{\psi}_{\mathrm{d}-}\right)^{*}\underline{I}_{\mathrm{q}-}\right\}. \tag{35}$$

The total average cage torque will be defined as

$$T_{(\mathrm{avg})} = T_{(\mathrm{cage})+} + T_{(\mathrm{cage})-}. \tag{36}$$

Figs. 4 and 5 show the corresponding equivalent circuits of the two fictitious stator-balance motors employed for cage

torque computation when positive sequence and negative sequence, respectively are considered. Note that for the case of a balanced poly-phase motor, only the positive sequence cage torque $T_{(\mathrm{cage})+}$ is present.

One drawback of the previously described equivalent circuits is that they employ fixed value parameters. The reactances, especially the *d-q* axes synchronous values ($X_\mathrm{d}, X_\mathrm{q}$) are subjected to strong saturation level. Saturation of the magnetic circuit is particularly complex in LSPMMs: different sections of the machine saturate independently, causing large and sometimes time-varying changes in equivalent circuit parameters such as inductances and back EMF (E_0). Therefore, the developed model used average saturated values for the *d-q* axes inductances and the open-circuit value for the back EMF.

A further improvement of the asynchronous cage torque computation is expected to be achieved by considering the space harmonics m.m.f. effects, not only the fundamental m.m.f. as in (34) and (35).

III. The Asynchronous Magnet Braking Torque

During asynchronous operation, the accelerating torque of the LSPM motor is the average cage torque minus the magnet braking torque and the load torque. The average cage torque is developed by "induction motor action", except that the saliency and the unbalanced stator voltages complicate the analysis and may compromise the performance.

The magnet braking torque is produced by the fact that the magnet flux generates currents in the stator windings, and is associated with the loss in the stator circuit resistance. The variation of this torque with speed follows a pattern similar to that in the induction motor, but the per-unit speed takes the place of slip.

The magnet braking torque should not be confused with the synchronous "alignment" torque that arises at synchronous speed, even though the magnet braking torque is still present at synchronous speed and therefore diminishes output and efficiency.

A complete *d-q* axis analysis of the magnet braking torque for a 3-phase symmetrical LSPM motor is given in [4] and [16]. Expressions for determining the currents and the flux linkages due to the magnets and the magnet braking torque are determined accordingly for the unsymmetrical single-phase LSPM motor.

The 1-phase LSPMM exhibits asymmetries on both stator and rotor. Thus the usage of *d-q* theory may be employed if we use the following assumptions: a) the stator windings have the same copper weight ($R_\mathrm{s} = R_\mathrm{m} = \beta^2 R_\mathrm{a}$, $X_\mathrm{ls} = X_\mathrm{lm} = \beta^2 X_\mathrm{la}$, $\mathrm{d_a} = \beta^{1/2}\mathrm{d_m}$); b) the capacitor impedance may be included in one of the synchronous reactance branches (i.e., X_d or X_q); c) the main and auxiliary windings circuits are associated with d-axis and q-axis respectively.

We can write the following voltage equations in rotor reference frame, with all variables referred to the main winding, considering the stator windings as short-circuited and neglecting the supply system impedance:

$$0 = R_\mathrm{s} I_\mathrm{dm} - j\omega \cdot (1-s) \cdot \psi_\mathrm{qm} \tag{37}$$

$$0 = R_\mathrm{s} I_\mathrm{qm} + j\omega \cdot (1-s) \cdot \psi_\mathrm{dm}. \tag{38}$$

Consequently, we obtain the flux-linkage expressions

$$\psi_\mathrm{dm} = \frac{X_\mathrm{d} I_\mathrm{dm} + E_0}{\omega} \tag{39}$$

$$\psi_\mathrm{qm} = \frac{(X_\mathrm{q} - X_\mathrm{C}) \cdot I_\mathrm{qm}}{\omega}. \tag{40}$$

Substituting (39) and (40) in (37) and (38) the currents are defined as

$$I_\mathrm{dm} = \frac{-(1-s)^2 \cdot (X_\mathrm{q} - X_\mathrm{C})}{R_\mathrm{s}^2 + X_\mathrm{d}(X_\mathrm{q} - X_\mathrm{C})(1-s)^2} \cdot E_0 \tag{41}$$

$$I_\mathrm{qm} = \frac{-(1-s) R_\mathrm{s}}{R_\mathrm{s}^2 + X_\mathrm{d}(X_\mathrm{q} - X_\mathrm{C})(1-s)^2} \cdot E_0. \tag{42}$$

The average air-gap magnet braking torque will be defined as

$$T_\mathrm{m} = \frac{P}{2} \cdot \left[\frac{1}{\beta} \cdot \psi_\mathrm{dm} I_\mathrm{qm} - \beta \cdot \psi_\mathrm{qm} I_\mathrm{dm} \right]. \tag{43}$$

However, a more accurate analytical model may be required for the magnet braking torque when the copper weight and distribution of the stator windings exhibit important differences. A literature survey [13], [17], [21]–[23], [26] shows that even using numerical analysis, the exact magnet braking torque prediction has not yet been achieved.

The average air-gap resultant electromagnetic torque will be given by

$$T_\mathrm{e} = T_{(\mathrm{avg})} + T_\mathrm{m}. \tag{44}$$

IV. The Asynchronous Pulsating Torques

In a LSPM motor the magnet alignment torque has a nonzero average value (i.e., averaged over one revolution or electrical cycle) only at synchronous speed [6], [16], [18]. At all other speeds it contributes an oscillatory (pulsating) component of torque. As the rotor approaches synchronous speed, the screening effect of the cage becomes less, and as the slip is very small, the pulsating torques cause large variations in speed that may impair the ability to synchronize large-inertia loads.

Analysis of the LSPM motor is made using the rotor reference frame and the *rotor current* components correspond to two induced currents and the equivalent current that is determined by the permanent magnet. Their frequencies are: a) sf harmonic, represented by the positive cage sequence; b) $(2-s)f$ harmonic, represented by the negative cage sequence; c) 0, represented by the permanent magnet equivalent current.

In the rotor reference frame the asynchronous operation as an induction motor and the influence of the permanent magnets determine the *stator current* components. Their frequencies are: a) the fundamental (f) represented by the positive forward and negative backward sequence cage component; b) $(1-2s)f$ harmonic, represented by the positive backward cage sequence; c) $(3-2s)f$ harmonic, represented by the negative forward cage component; d) $(1-s)f$ harmonic, represented by the induced stator currents due to the magnet rotation. These harmonics interact and determine several pulsating torques [1], [2].

The interaction between the *rotor current* components determines four cage pulsating torque components and two permanent pulsating torque components [2]. We may classify the

TABLE I
STATOR WINDING DATA

# Motor	Winding parameters		
	N_m [p.u.]	β	d_m/d_a
Motor 1	1.46	1.42	1.22
Motor 2	1.14	1.42	1.3
Motor 3	1	1	1
Motor 4	0.87	0.70	0.76

amplitude (zero to peak) of the fundamental pulsating torques according to their main cause in: reluctance, unbalanced stator voltage and permanent magnet (excitation) pulsating torques

Reluctance pulsating torques

$$T_{(\mathrm{pls})(2sf)}=\frac{P}{2}\cdot\mathrm{Abs}\left\{\left(\underline{\psi}_{\mathrm{q}+}\right)\underline{I}_{\mathrm{d}+}-\left(\underline{\psi}_{\mathrm{d}+}\right)\underline{I}_{\mathrm{q}+}\right\} \quad (45)$$

$$T_{(\mathrm{pls})(4-2s)f}=\frac{P}{2}\cdot\mathrm{Abs}\left\{\left(\underline{\psi}_{\mathrm{q}-}\right)\underline{I}_{\mathrm{d}-}-\left(\underline{\psi}_{\mathrm{d}-}\right)\underline{I}_{\mathrm{q}-}\right\}. \quad (46)$$

Unbalanced stator voltage pulsating torques

$$T_{(\mathrm{pls})(2f)}=\frac{P}{2}\cdot\mathrm{Abs}\left\{\left(\underline{\psi}_{\mathrm{q}+}\right)\underline{I}_{\mathrm{d}-}-\left(\underline{\psi}_{\mathrm{d}+}\right)\underline{I}_{\mathrm{q}-}\right\} \quad (47)$$

$$T_{(\mathrm{pls})(2-2s)f}=\frac{P}{2}\cdot\mathrm{Abs}\left\{\left(\underline{\psi}_{\mathrm{q}-}\right)\underline{I}_{\mathrm{d}+}-\left(\underline{\psi}_{\mathrm{d}-}\right)\underline{I}_{\mathrm{q}+}\right\}. \quad (48)$$

Permanent magnet (excitation) pulsating torques

$$T_{(\mathrm{pls})(sf)}=\frac{P}{2}\cdot\mathrm{Abs}\left[\left(\underline{\psi}_{\mathrm{q}+}\right)I_{\mathrm{dm}}+(\psi_{\mathrm{qm}})\underline{I}_{\mathrm{d}+}\right]-\frac{P}{2}\cdot\mathrm{Abs}\left[\left(\underline{\psi}_{\mathrm{d}+}\right)I_{\mathrm{qm}}+(\psi_{\mathrm{dm}})\underline{I}_{\mathrm{q}+}\right] \quad (49)$$

$$T_{(\mathrm{pls})(2-s)f}=P\cdot\mathrm{Abs}\left[\left(\underline{\psi}_{\mathrm{q}-}\right)I_{\mathrm{dm}}+(\psi_{\mathrm{qm}})\underline{I}_{\mathrm{d}-}\right]-P\cdot\mathrm{Abs}\left[\left(\underline{\psi}_{\mathrm{d}-}\right)I_{\mathrm{qm}}+(\psi_{\mathrm{dm}})\underline{I}_{\mathrm{q}-}\right]. \quad (50)$$

Note that while for the reluctance and excitation pulsating torques their total effect is given by their sum, for the unbalanced stator pulsating torque the total effect is given by their difference. Also, the permanent magnet (excitation) pulsating torque varies with the number of poles (P) whilst the other pulsating torque components depend on the number of pole-pairs.

V. EXPERIMENTAL AND SIMULATION RESULTS

The experiments were performed on four motor types, equipped with identical rotors and stator laminations, but with different stator windings [1]. Table I presents the stator winding data for the tested motors. Note that the assumption made in Section III is valid only for motors 3 and 4. The investigation includes two other motors (1 and 2) with a different copper weight in the stator windings. In this way it is possible to observe the influence of this simplification on the simulations, when compared to a wide spectrum of experimental data.

The simulation results are presented for the case when two capacitors were used, 23 μF at low speed and 3 μF at high speed (above 80–90% of synchronous speed), for all the analyzed LSPM motor types. Note that these values do not correspond to the optimum values of any of the analyzed motors. At low speed the torque oscillations make any steady-state measurements with standard equipment impossible.

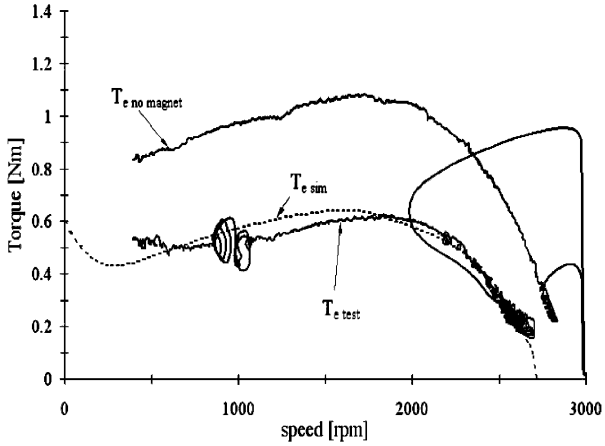

Fig. 6. Experimental and computed torque variation vs. speed during asynchronous no-load operation, Motor 1.

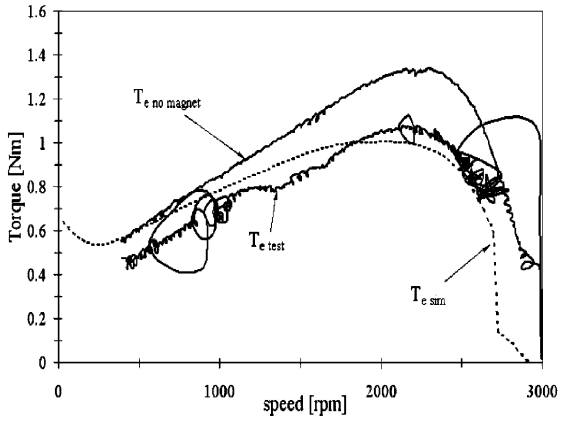

Fig. 7. Experimental and computed torque variation vs. speed during asynchronous no-load operation, Motor 2.

A trade-off has to be made depending on the application: lower starting torque and efficiency, but increased load torque and synchronization capability (Motor 2); higher starting torque and efficiency, but decreased load torque and synchronization capability (Motor 1 and 3); higher starting and load torque and synchronization capability, but lower efficiency and higher magnetic noise i.e., pulsating torques (Motor 4). The magnet braking torque exhibits a maximum in the range of 0.25 Nm (Motor 2) to 0.65 Nm (Motor 4). The cage torque in all the cases overcomes the magnet braking torque.

Figs. 6–9 illustrate the experimental quasi steady-state torque variation vs. speed during no-load operation for a line-start permanent magnet motor, supplied with an unbalanced stator voltage system, with a capacitor-start value of 23 μF. An hysteresis brake (coupled with an acquisition and control system) was used to test the motor. The automatic procedure starts running the motor without load, then gradually decreases the speed measuring at each step the torque and power. The solid line represent the experimental data values that were measured when the rotor was not equipped with permanent magnets ($T_{(\mathrm{e\ no\ magnets})}$), and when the motor was equipped with permanent magnets (the experimental data for the average resultant torque – $T_{(\mathrm{e\ test})}$). The capacitor value was not optimized, as

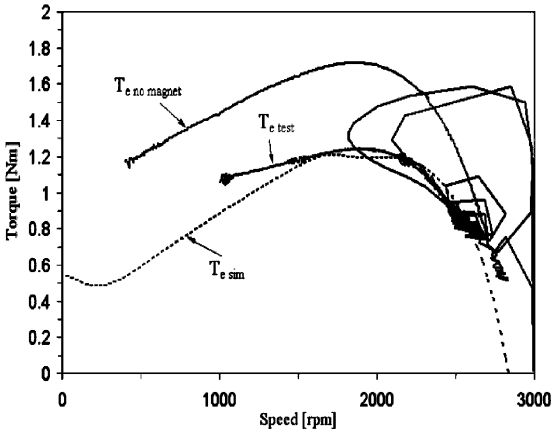

Fig. 8. Experimental and computed torque variation vs. speed during asynchronous no-load operation, Motor 3.

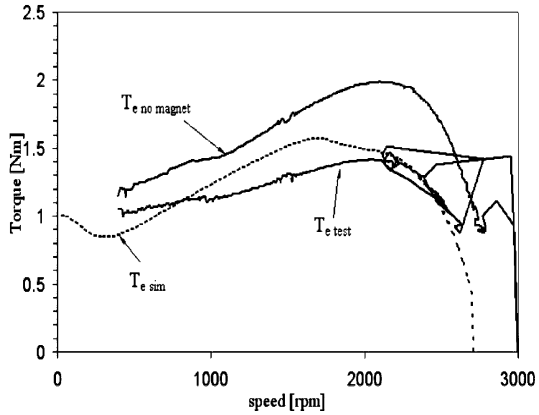

Fig. 9. Experimental and computed torque variation vs. speed during asynchronous no-load operation, Motor 4.

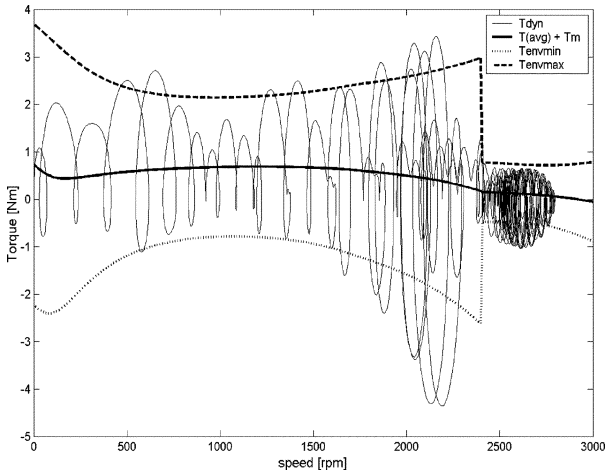

Fig. 10. Computed dynamic, resultant torque and envelope with pulsating components variation vs. speed during no-load starting operation – Motor 1.

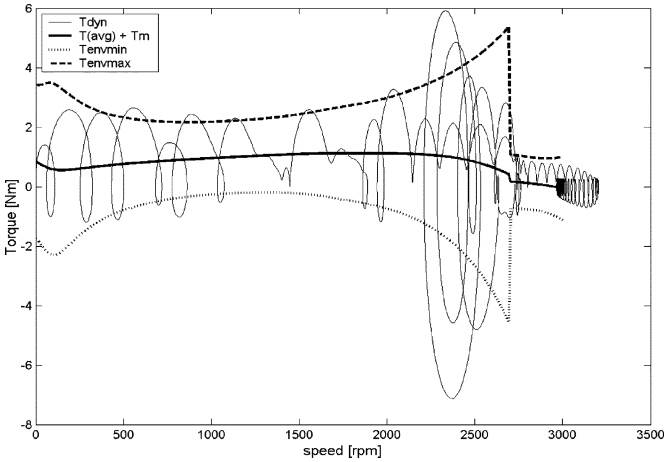

Fig. 11. Computed dynamic, resultant torque and envelope with pulsating components variation vs. speed during no-load starting operation – Motor 2.

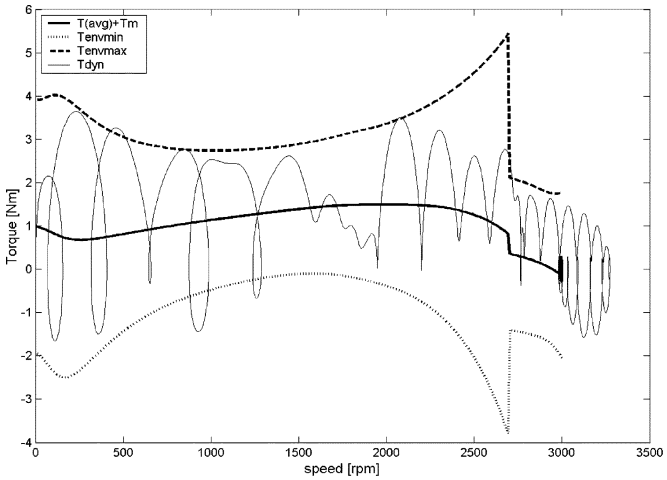

Fig. 12. Computed dynamic, resultant torque and envelope with pulsating components variation vs. speed during no-load starting operation – Motor 3.

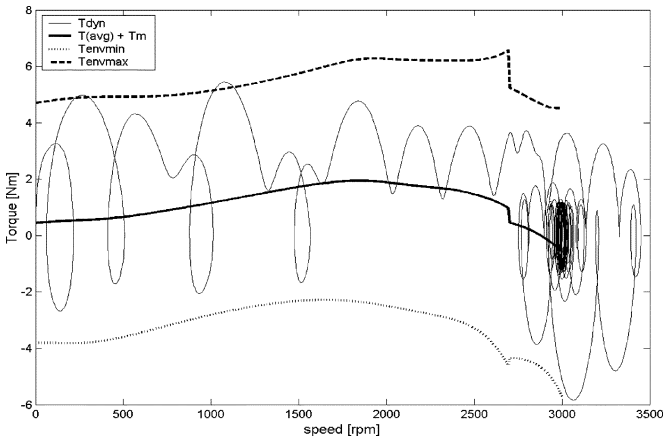

Fig. 13. Computed dynamic, resultant torque and envelope with pulsating components variation vs. speed during no-load starting operation – Motor 4.

the experiments were intended to study the torque behavior during starting operation for the same capacitance values and different stator windings data. The average electromagnetic torque $T_{(\mathrm{e\ sim})}$ computed with (44) is graphically presented by the dotted lines in Figs. 6–9. Note the best agreement was obtained for motor 3 (identical stator windings – $\beta = 1$)

In Figs. 10–13, the computed dynamic torque and quasisteady state average resultant torque (solid line) and the envelope of the instantaneous torque are presented (dashed lines). Note the torque behavior at the asynchronous operation when the auxiliary capacitive impedance ($\underline{Z}_{\mathrm{C}}$) is switched from the capacitor-start to the capacitor-run fixed value. The dynamic torque (T_{dyn}) simulation pattern follows that described in [3], [6]. The minimum and maximum envelope trajectory ($T_{\mathrm{envmax}}, T_{\mathrm{envmin}}$) are obtained by superimposing the effect of the pulsating torque

components effect over the average resultant torque. This approach neglects the mechanical pulsation due to rotor/load inertia and assumes that even though pulsating torque components vary with different frequencies, their global effect may be simulated by superposition. The slight difference between the quasi steady-state torque and dynamic torque is due to the rotor inertia influence and the pulsating torque variation with frequency harmonics. All simulations have been implemented neglecting saturation and core losses. However, the proposed model may include nonlinear effects (e.g., core loss modeling through a nonlinear resistor coupled in parallel with the magnetising reactance).

VI. Characteristics of Asynchronous Torque Components

For the average *asynchronous cage torque components*, the main observations are:

a) A higher starting torque would require a high-resistance rotor cage, but this feature will present the classical "dip" at half synchronous speed, in a similar way to the Goerges phenomenon in induction motors with an unsymmetrical rotor [8]. This "dip" can be minimized by using lower resistance rotor bars, or almost symmetrical cage rotors, i.e., $R_{\rm rd} \approx R_{\rm rq}$. Therefore, an optimum value for the cage rotor resistance must be employed.

b) The negative sequence torque can be minimized by using a minimum admissible value for the stator resistance. However, this task is hard to achieve for small motors ($P_{\rm n} < 1$ kW).

c) The minimization of negative sequence voltage amplitude toward zero can be made for a specific operation point (speed, load) by using a correct choice for the start- or run-capacitor [3].

d) It is of interest that the developed airgap cage torque at synchronous speed is not zero as in a symmetrical induction motor. The cage torque of the asymmetrical PM machine at $s = 0$ is always *negative*. The only exception is when the saliency effect can be neglected $X_{\rm d} \approx X_{\rm q}$, and the stator currents are balanced (negative sequence voltage $\underline{V}_{-} = 0$). This nonzero average cage torque at synchronous speed does not depend on the cage parameters (resistance or leakage reactance). This is the effect of the rotor saliency and the fact that the stator resistance cannot be neglected for fractional horsepower AC motors such as the analyzed motor. The air-gap cage torque should not be confused with the negative sequence torque that is characteristic of an unbalanced 1-phase LSPM motor that runs at synchronous speed [30].

For the *asynchronous magnet braking torque*, the main observations are:

a) The capacitive impedance that is connected in series with the auxiliary winding may lead to a minimization of the magnet braking torque when its value is much higher than the synchronous reactances; At certain speed levels a resonance phenomenon may occur that will determine important oscillations during the starting period.

b) The minimization of the magnet braking torque can be obtained through different constructive methods: less magnet material, increased airgap. However, all the constructive methods that lead to a diminished magnet braking torque are usually reflected in lower efficiency at synchronous speed.

c) A simple measurement method for the magnet braking torque can be implemented by short-circuiting the stator windings (with the capacitive impedance included in the auxiliary circuit). The LSPM motor is driven with a load motor (e.g., DC or hysteresis brake) at different speeds. Consequently, the magnet braking torque can be measured directly at the motor shaft.

For the *pulsating torque components*, the main observations are:

a) The asymmetries on both stator and rotor determine six important pulsating torque components for the run-up period [$2sf$, $2f$, $(2-2s)f$, $(4-2s)f$, $(2-s)f$, sf] and two components for the synchronous operation [$2f$, $4f$], compared to two and zero components respectively for the 3-phase symmetrical motor case [1], [2], [4].

b) Even for a symmetrical rotor (i.e., d-q axis parameters are identical), the pulsating excitation and unbalanced stator torque components will not disappear completely. The unsymmetrical stator pulsating torque components ($2f$ and $(2-2s)f$) are always present for an unbalanced stator voltage system. The double frequency pulsating torque component represents the main cause of pulsating for the single-phase LSPM motor. This component is characteristic of any 1-phase AC motor: induction, synchronous reluctance, or synchronous permanent magnet. At synchronous speed the fundamental pulsating torques will vary with $2f$ and $4f$ frequency.

c) The forward sequence excitation pulsating component is responsible for larger pulsations especially at low speed, whilst the negative sequence excitation pulsating component has a comparable value with the reluctance pulsating torque components

d) The reluctance pulsating torque components [$2sf$ and $(4-2s)f$] are entirely dependent on the machine parameters (resistances and reactances). The difference between the rotor d-q axis resistances and the leakage reactances determines an increased pulsating "dip" torque around the half-synchronous speed region. The difference between the d-q axis magnetization reactances determines an increased pulsating torque around the synchronous speed region.

e) The rotor asymmetry is responsible for the nonzero reluctance pulsating torque at standstill, and the stator asymmetry is responsible for the nonzero unbalanced stator pulsating torque even at synchronous speed operation. For a single-phase permanent magnet motor, the proper selection of a capacitor to obtain a balanced stator voltage system will lead only to the minimization of the stator asymmetry effect. The rotor asymmetry effect cannot be eliminated.

VII. Conclusions

The asynchronous performance prediction for a line start permanent magnet motor can be made assuming that asynchronous cage torques and magnet braking torque effects can be superimposed. Obviously, the superposition principle will neglect the circuit cross-couplings. Important information about the motor torque capability is obtained through the study of different torque components. The deduced torque expressions may be extended for the general case of the m-phase AC motor, supplied with unbalanced stator voltage.

References

[1] M. Popescu, T. J. E. Miller, M. I. McGilp, G. Strappazzon, N. Trivillin, and R. Santarossa, "Line start permanent magnet motor: Single-phase starting performance analysis," in *Proc. Conf. Rec. IEEE Ind. Appl. Soc. Annual Meeting* , vol. 4, Pittsburgh, PA, Oct. 13–18, 2002, pp. 2499–2506.

[2] T. J. E. Miller, M. Popescu, and M. I. McGilp. Asynchronous performance analysis of a single-phase capacitor run permanent magnet motor. presented at Proc. Conf. Rec. Int. Conf. Electrical Machines

[3] T. J. E. Miller, "Single-phase permanent magnet motor analysis," *IEEE Trans. Ind. Appl.*, vol. IA-21, no. 3, pp. 651–658, May/Jun. 1985.

[4] V. B. Honsinger, "Permanent magnet machine: Asynchronous operation," *IEEE Trans. Power App. Syst.*, vol. PAS-99, no. 7, pp. 1503–1509, Jul. 1980.

[5] ——, "Performance of polyphase permanent magnet machines," *IEEE Trans. Power App. Syst.*, vol. PAS-99, no. 7, pp. 1510–1518, Jul. 1980.

[6] T. J. E. Miller, "Synchronization of line-start permanent magnet motors," *IEEE Trans. Power App. Syst.*, vol. PAS-103, no. 7, pp. 1822–1828, Jul. 1984.

[7] C. Concordia, *Synchronous Machines*. New York: Wiley, 1951.

[8] H. L. Gabarino and E. T. B. Gross, "The goerges phenomenon – Induction motors with unbalanced rotor impedances," *AIEE Trans.*, vol. 69, pp. 1569–1575, 1950.

[9] K. Miyashita, S. Yamashita, S. Tanabe, T. Shimozu, and H. Sento, "Development of a high-speed 2-pole permanent magnet synchronous motor," *IEEE Trans. Power App. Syst.*, vol. PAS-99, no. 6, pp. 2175–2183, Nov./Dec. 1980.

[10] V. Honsinger, "The fields and parameters of interior type AC permanent magnet machines," *IEEE Trans. Power App. Syst.*, vol. PAS-101, no. 4, pp. 867–876, Apr. 1982.

[11] P. C. Krause, O. Wasynczuk, and S. Sudhoff, *Analysis of Electrical Machinery*. New York: IEEE Press, 1995.

[12] G. Slemon, *Magnetoelectric Devices*. New York: Wiley, 1966.

[13] S. Williamson and A. M. Knight, "Performance of skewed single-phase line-start permanent magnet motors," *IEEE Trans. Ind. Appl.*, vol. 35, no. 3, pp. 577–582, May/Jun. 1999.

[14] C. M. Stephens, G. B. Kliman, and J. Boyd, "A line-start permanent magnet motor with gentle starting behavior," in *Proc. 33rd Ind. Appl. Soc. Annual Meeting, Ind. Appl. Conf.*, vol. 1, 1998, pp. 371–379.

[15] B. J. Chalmers, G. D. Baines, and A. C. Williamson, "Performance of a line-start single-phase permanent-magnet synchronous motor," in *Proc. 7th Int. Conf. Elect. Mach. Drives*, 1995, pp. 413–417.

[16] M. A. Rahman and A. M. Osheiba, "Performance of large line-start permanent magnet synchronous motors," *IEEE Trans. Energy Convers.*, vol. 5, no. 1, pp. 211–217, Mar. 1990.

[17] A. M. Knight and C. I. McClay, "The design of high-efficiency line-start motors," *IEEE Trans. Ind. Appl.*, vol. 36, no. 6, pp. 1555–1562, Nov./Dec. 2000.

[18] H.-P Nee, L. Lefevre, P. Thelin, and J. Soulard, "Determination of d and q reactances of permanent-magnet synchronous motors without measurements of the rotor position," *IEEE Trans. Ind. Appl.*, vol. 36, no. 5, pp. 1330–1335, Sep./Oct. 2000.

[19] J. Soulard and H.-P. Nee, "Study of the synchronization of line-start permanent magnet synchronous motors," in *Proc. Industry Applications Conf. Rec.*, vol. 1, 2000, pp. 424–431.

[20] B. N. Chaudhari and B. G. Fernandes, "Synchronous motor using ferrite magnets for general purpose energy efficient drive," in *Proc. IEEE Region 10 Conf.*, vol. 1, 1999, pp. 371–374.

[21] A. M. Knight and S. Williamson, "Influence of magnet dimensions on the performance of a single-phase line-start permanent magnet motor," in *Proc. Int. Conf. Electric Machines Drives*, 1999, pp. 770–772.

[22] A. M. Knight and J. C. Salmon, "Modeling the dynamic behavior of single-phase line-start permanent magnet motors," in *Proc. 34th Industry Applications Society Annual Meeting. Conf.*, vol. 4, 1999, pp. 2582–2588.

[23] J. Cros and P. Viarouge, ""Modeling of the coupling of several electromagnetic structures using 2D field calculations" Magnetics," *IEEE Trans. Magn.*, pt. 1, vol. 34, no. 5, pp. 3178–3181, Sep. 1998.

[24] B. N. Chaudhari, S. K. Pillai, and B. G. Fernandes, "Energy efficient line start permanent magnet synchronous motor," in *Proc. IEEE Region 10 Int. Conf. Global Connectivity in Energy, Computer, Communication Control*, vol. 2, 1998, pp. 379–382.

[25] K. J. Binns, "Permanent magnet machines with line start capabilities: Their design and application," in *Proc. Inst. Elect. Eng. Permanent Magnet Machines Drives Colloq.*, 1993, pp. 5/1–5/5.

[26] R. Carlson, N. Sadowski, S. R. Arruda, C. A. Da Silva, and L. Von Dokonal, "Single-phase line-started permanent magnet motor analysis using finite element method," in *Proc. Industry Applications Society Annual Meeting Conf. Rec.* , vol. 1, 1994, pp. 227–233.

[27] R. Wu and G. R. Slemon, "A permanent magnet motor drive without a shaft sensor," *IEEE Trans. Ind. Appl.*, vol. 27, no. 5, pp. 1005–1011, Sep./Oct. 1991.

[28] A. Consoli, P. Pillay, and A. Raciti, "Start-up torque improvement of permanent magnet synchronous motors," in *Proc. Industry Applications Society Annual Meeting Conf. Rec.*, vol. 1, 1990, pp. 275–280.

[29] P. Pillay and P. Freere, "Literature survey of permanent magnet AC motors and drives," in *Proc. Industry Applications Society Annual Meeting Conf. Rec.*, vol. 1, 1989, pp. 74–84.

[30] I. Boldea, T. Dumitrescu, and S. Nasar, "Unified analysis of 1-phase AC motors having capacitors in auxiliary windings," *IEEE Trans. Energy Convers.*, vol. 14, no. 3, pp. 577–582, Sep. 1999.

[31] S. Yamamoto, T. Ara, S. Oda, and K. Matsuse, "Prediction of starting performance of PM motor by DC deacy testing method," in *Proc. Industry Applications Society Annual Meeting Conf. Rec.*, vol. 4, 1999, pp. 2574–2581.

[32] A. Consoli and A. Racitti, "Analysis of permanent magnet synchronous motors," *IEEE Trans. Ind. Appl.*, vol. 27, no. 2, pp. 350–354, Mar./Apr. 1991.

[33] T. Sebastian, G. R. Slemon, and M. A. Rahman, "Modeling of permanent magnet synchronous motors," *IEEE Trans. Magn.*, vol. MAG –22, no. 5, pp. 1069–1071, Sep. 1986.

[34] C. R. Steen, "Direct Axis Aiding Permanent Magnets for a Laminated Synchronous Motor Rotor," U.S. Patent #4 139 790, Feb. 1979.

[35] G. B. Kliman, M. A. Preston, and D. W. Jones, "Permanent Magnet Line Start Motor Having Magnets Outside the Starting Cage," U.S. Patent #5 548 172, Aug. 1996.

[36] Miyashita *et al.*, "Stress Protection for Permanent Magnet Type Synchronous Motor," U.S. Patent #4 144 469, Aug. 1977.

[37] G. Ray and J. B. Gollhardt, "Permanent Magnet Motor Armature," U.S. Patent #4 322 648, Mar. 1980.

[38] K. Mikulic, "Rotor Lamination for an AC Permanent Magnet Synchronous Motor," U.S. Patent #5 097 166, Sep. 1990.

Mircea Popescu (M'98–SM'04) was born in Bucharest, Romania. He received the M.Eng. and Ph.D. degrees in electrical engineering from the University "Politehnica" Bucharest, Romania.

Since 2000, he has been a Research Associate with SPEED Laboratory, Glasgow University, Glasgow, U.K. From 1984 to 1986, he worked on dc drives design and quality testing at "Electrotehnica" S.A. Bucharest. From 1986 to 1997, he was a Project Manager with the Research Institute for Electrical Machines (ICPE-ME), Bucharest, working on industrial and research development. From 1991 to 1997, he cooperated as a Visiting Assistant Professor, Electrical Drives and Machines Department, University "Politehnica" Bucharest. From 1997 to 2000, he was a Research Scientist with the Electromechanics Laboratory, Helsinki University of Technology, Espoo, Finland.

T. J. E. Miller (M'74–SM'82–F'96) received the M.Sc. degree from the University of Glasgow, Glasgow, U.K., and the Ph.D. degree in electrical engineering from Leeds University.

From 1979 to 1986, he was an Electrical Engineer and Program Manager with GE Research and Development, Schenectady, NY, and his industrial experience includes time with GEC (U.K.), British Gas, International Research and Development, and a student-apprenticeship with Tube Investments Ltd. He is Professor of Electrical Power Engineering and Founder and Director of the SPEED Consortium at the University of Glasgow. He is the author of more than 100 publications in the fields of motors, drives, power systems, and power electronics, including seven books.

Dr. Miller is a Fellow of the IEE.

Malcolm McGilp was born in Helensburgh, U.K. He received the B.Eng. degree (Hons.) in electronic systems and microcomputer engineering, University of Glasgow, Glasgow, U.K.

Currently, he is a Research Associate in the SPEED Laboratory, University of Glasgow, where he was a Research Assistant from 1987 to 1996. He is responsible for the software architecture of the SPEED motor design software and has developed the interface and user facilities which allow it to be easy to learn and integrate with other PC-based software.

Giovanni Strappazzon graduated from the Padua University, Padua, Italy, in 1998.

Currently, he is a Researcher on innovative motors for Zanussi Elettromeccanica, Comina, Italy. He also worked for a factory that manufactured small synchronous motors mainly for aquarium pumps.

Mr. Strappazzon won an award as Researcher in the Department of Electrical Engineering for the optimization in design of electrical motors in 1999.

Nicola Trivillin was born in Pordenone, Italy, in 1970. He received the "laurea" in electrical engineering from Padua University, Padua, Italy, in 1995 with a thesis on finite-element analysis of single phase induction motor with auxiliary phase.

Currently, he is Manager of the Electrical Competence Center within Zanussi Elettromecanica, Comina, Italy. He was Electric Motor Specialist when he joined the Research and Design Department.

Roberto Santarossa was born in 1969 in Pordenone, Italy. He received the electrical engineering degree from the University of Padua, Padua, Italy, in 1996, with a thesis about voltage stability of large electric power systems.

Currently, he is Electric Motor Designer with Zanussi Elettromeccanica, Comina, Italy, dealing with design and development of fractional horsepower motors. He has been with Zanussi Elettromeccanica since 1997.